THE BALTIC JOURNAL
OF ROAD AND BRIDGE ENGINEERING

ISSN 1822-427X print / ISSN 1822-4288 online
2014 Volume 9(2): 101–107

STRAINS IN ASPHALT PAVEMENTS UNDER CIRCULAR AND RECTANGULAR FOOTPRINTS

Massimo Losa[1]✉, Andrea Di Natale[2]

[1]*Dept of Civil and Industrial Engineering, University of Pisa, Largo Lucio Lazzarino, 1–56122 Pisa, Italy*
[2]*NExT Ltd, Viale Rinaldo Piaggio, 32–56025 Pontedera, Italy*
E-mails: [1]*losa@ing.unipi.it;* [2]*andrea.dinatale@next-lab.it*

Abstract. The analysis of flexible pavements is usually carried out by the Linear Elastic Theory in axial-symmetric configuration, and by assuming that stresses are uniformly distributed over a circular footprint. The application of these methods requires simple computations, but beside this, the approximation of the real geometry with circular footprints causes erroneous results in the stress-strain response and therefore in the damage analysis. Rectangular footprint is closer to the real shape of the tire/pavement contact area. This paper aims to identify some relations to evaluate the effective strains induced in pavements by rectangular footprint loads by considering an equivalent single or group of circular footprints. In order to achieve this goal, pavement response was evaluated for different variable combinations both by ViscoRoute 2.0 software for the rectangular footprint, and by an elastic model for the circular footprint in axial-symmetric configuration; results obtained by the two analyses were compared in order to develop two different models. The first model proposes a correction coefficient λ of the radius of the circular area to be used for calculating strains beneath the centre of the rectangular footprint. The correction coefficient λ calculated for different variable configurations were related to those variables regarded as significant by means of a multivariate regression. In the second model, in order to calculate strains outside the rectangular footprint, the superposition of circular footprints that better approximates the rectangular ones was determined.

Keywords: rectangular footprint, circular footprint, multi-layered elastic analysis, flexible pavements.

1. Introduction

In order to correctly evaluate performances of asphalt pavements, such as rutting and fatigue resistance, an accurate computation of vertical and transversal critical strains due to representative loads and environmental conditions is required. For existing pavements, critical strains are obtained by using results of deflection measurements carried out by the Falling Weight Deflectometer; some relationships were developed to calculate critical strains induced in pavements by the circular load plate as a function of deflection parameters (Losa *et al.* 2008). As far as the design of new pavements is concerning, strains are calculated by mechanistic analysis of pavements. According to the most common methods used in pavement design, including the Mechanistic-Empirical Pavement Design Guide (MEPDG) method, the stress-strain state is computed under linear elastic axial-symmetric conditions, by considering circular-shaped footprints and the tire/pavement contact stress uniformly distributed over pavement. Even if these methods are relatively simple and fast, the assumptions adopted lead to not negligible errors in strain calculation, and so, in damage prediction (Blab 1999; De Beer, Fisher 1997; Hajj *et al.* 2012; Novak *et al.* 2003; Park *et al.* 2005a, 2005b; Wang, Machemehl 2006; Weissman 1999; Yue, Svec 1995).

These errors are linked to two approximations:

a) the real footprint shape;

b) the non-uniform contact stress.

This paper is focused on the first issue.

In order to make the load model closer to reality, Yoder and Witczak as well as Huang propose a specific size of the equivalent footprint for both the oval and the rectangular shapes. Alkasawneh *et al.* (2008) demonstrates that different footprint configurations, including the ones already mentioned, bring to significant differences in pavement response.

The simulations performed in this study support this issue. Fig. 1 shows the conventional reference frame adopted in this work. The results obtained point out that under equal load P, kN, and footprint area A, m^2 (therefore equal stress) the use of a circular footprint,

doi:10.3846/bjrbe.2014.13

rather than a rectangular one, determines an error Δ, %, in computed strains which ranges between 50–100% for longitudinal strain ε_x and transversal strain ε_y values, and which is about 10% for the vertical strain ε_z values. If the longer side of the rectangle is oriented along the x direction, the utilization of a circular footprint leads to underestimate the ε_y values and to overestimate both the ε_x and ε_z values.

The error is maximum for strains computed under the loading area and close to it, whereas it tends to be negligible for distances between 0.4–0.5 m away from the footprint. In fact, around this distance only the load force becomes significant being the effect of load geometry negligible.

2. Aims and methodology of the study

This study aims to determine a set of relationships to predict strains induced by any rectangular-shaped footprint by using strains induced by a single or an overlap of circular-shaped footprints.

In order to determine these relationships, different pavement configurations, obtained by changing layer thickness and modulus, and rectangular footprint sizes were considered. For each of these, the linear elastic strains were computed at different depths of the asphalt concrete multi-layers. The strains induced by rectangular footprints in the elastic multilayer were computed with the ViscoRoute 2.0 software (Chabot *et al.* 2010), while the strains induced by circular footprints were calculated with a linear elastic model in axial-symmetric configuration. Preliminarily, it was checked that under the same circular load σ, kPa, and at any depth z, m not significant differences exist between the pavement response of the ViscoRoute 2.0 and that of the linear elastic model in axial-symmetric configuration.

The ViscoRoute 2.0 software uses a semi-infinite multi-layer model of the pavement structure that is composed of horizontal layers in the z-direction. Each layer of the pavement structure is homogeneous. The structure is loaded by one or several loads moving in the x-direction with a certain constant speed. The load is applied in any of the three directions, at the free surface (z = 0) of the system. The load is either punctual or uniformly distributed on a rectangular or an elliptical surface area. The mechanical behaviour of the materials is assumed to be either linear elastic or linear thermo-viscoelastic. In the first case, the mechanical properties are defined by the Young modulus E and the Poisson ratio ν. In the second case, the behaviour is represented by the five viscoelastic coefficients of the Huet-Sayegh model that can be determined by the procedure reported by Losa, Di Natale (2014). A complete model description is reported by Duhamel *et al.* (2005).

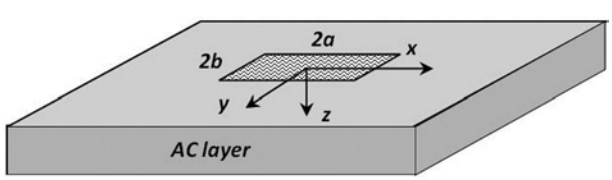

Fig. 1. Dimensions of the rectangular footprint and reference axes

For the purposes of this work, only the linear elastic feature of the software was used, with the representative loading frequency evaluated by the procedure proposed by Losa, Di Natale (2012).

3. Model for the equivalent circular footprint calculation

3.1. Strains beneath the centre of the rectangular footprint

For each configuration considered, the strains induced by the rectangular footprint, at different depths of the asphalt concrete layers were calculated along the central vertical axis (z axis). Subsequently, the radius of the circular-shaped footprint that produces, for the same uniform vertical contact stress, the same strain values along its central axis was computed. Since this, it becomes possible to modify the radius of the circular footprint, whose area is the same of the rectangular-shaped one, through the following formula (1):

$$r = \lambda \sqrt{\frac{4ab}{\pi}}, \quad (1)$$

where r – equivalent circular footprint radius, m; λ – correction coefficient; a, b – principal axes of the rectangular footprint, m.

Simulations were carried out on a pavement model composed of a single asphalt concrete layer and a sub base course over the subgrade. The method proposed by Cohen was applied to determine the minimum required sample size for a multiple regression study, given the desired probability level p, the number of predictors in the model n, the anticipated effect size f^2, and the desired statistical power level π. The anticipated effect size f^2 was assumed equal to 0.35 (by convention, large effect), whereas the statistical power level π = 80%, the p-value p = 5% and the number of predictors n = 4 ($\frac{a}{b}$, s_{AC}, E_{AC}, z). The application of this method shows that the sample must consist of at least 39 combinations. In order to calibrate the model coefficients, 42 configurations were obtained by combining the following parameters:

– five pavement structures with different layer thickness and asphalt concrete modulus;

– three investigation depths (at $\frac{1}{2}s$, $\frac{3}{4}s$ and s, where s – the thickness of the asphalt concrete layer, m);

– six different-sized rectangular footprints.

Table 1 shows the parameters used to obtain the 42 ombinations.

The single tire load was assumed constant P = 30 kN, while stresses were changed with the parameter a. Through the simulations, it was established that:

1) the sub base modulus in the range considered has negligible influence on the correction coefficient λ;

2) the asphalt concrete stiffness modulus E_{AC}, MPa in the range considered has very scanty influence on the

correction coefficient λ. For example, by using the correction coefficient λ calculated for E_{AC} = 13 000 MPa in a pavement with E_{AC} = 2000 MPa, the strain error Δ, %, is lower than 2%;

3) two pavements with different thickness *s*, at the same depth *z,* and with all the other conditions being equal, provide the same correction coefficient λ. Thus the correction coefficient λ depends on *z* and not on the ratio $\frac{z}{s}$;

4) different-sized rectangular footprints characterized by the same ratio $\frac{a}{b} \geq 1$, produce the same correction coefficient λ, which therefore depends on $\frac{a}{b}$ and not individually on *a* and *b*;

5) three strains ε_x, ε_y, ε_z require different correction coefficients λ.

The plot of the correction coefficients λ versus one variable at a time, by holding all the other variables constant, shows the function $\lambda\left(\frac{a}{b}, z\right)$ is convex. Therefore, a multivariate linear regression cannot be applied directly to these variables, but a variable transformation obtained by combining linear and quadratic forms of $\frac{a}{b}$ and *z* must be introduced.

By proceeding iteratively, the least significant variables (calculated with the *t*-Student test) were disregarded at each time and new regression coefficients were determined, until the 95% level of significance was obtained for all the remaining variables. The equivalent circular footprint radius to be used for strain calculations along the three main directions *x*, *y*, *z* is determined by the following formulas (2, 3, 4):

Table 1. Parameters used in simulations and range of variation

Parameter		Range of values	Description
Symbol	Unit		
a	m	0.075–0.18	Half-length of the rectangular footprint (direction *x*)
b	m	0.045–0.18	Half-width of the rectangular footprint (direction *y*)
s_{AC}	m	0.15–0.30	Asphalt concrete layer thickness
E_{AC}	MPa	7725–17 230	Elastic modulus of the asphalt concrete layer
s_{BA}	m	0.30	Sub base course thickness
E_{BA}	MPa	250–350	Elastic modulus of the sub base course
E_{SUBG}	MPa	120	Elastic modulus of the subgrade
z	m	$0.5s_{AC}$–s_{AC}	Depth at which the strains are calculated

Table 2. Statistical parameters of correction coefficients λ_x, λ_y, λ_z

Correction coefficient	Variable	Coefficient	Standard error	Standard error of the estimate	R^2 of the estimate
λ_x	$\frac{a}{b}$	0.2896	$2.719 \cdot 10^{-3}$	$7.884 \cdot 10^{-3}$	0.996
	constant	0.714	$4.381 \cdot 10^{-3}$		
λ_y	$\frac{a}{b}$	–0.1962	$1.245 \cdot 10^{-2}$	$12.561 \cdot 10^{-3}$	0.949
	$z\left(\frac{a}{b}\right)^2$	0.2082	$3.271 \cdot 10^{-5}$		
	$\frac{a}{b}z^2$	–0.4623	$1.483 \cdot 10^{-3}$		
	constant	1.180	$1.303 \cdot 10^{-2}$		
λ_z	$\frac{a}{b}$	0.1453	$4.987 \cdot 10^{-2}$	$9.241 \cdot 10^{-3}$	0.939
	$\left(\frac{a}{b}\right)^2$	–0.06386	$1.711 \cdot 10^{-2}$		
	$z\left(\frac{a}{b}\right)^2$	0.2713	$2.521 \cdot 10^{-5}$		
	$\frac{a}{b}z^2$	–0.8887	$1.170 \cdot 10^{-7}$		
	constant	0.9081	$3.387 \cdot 10^{-2}$		

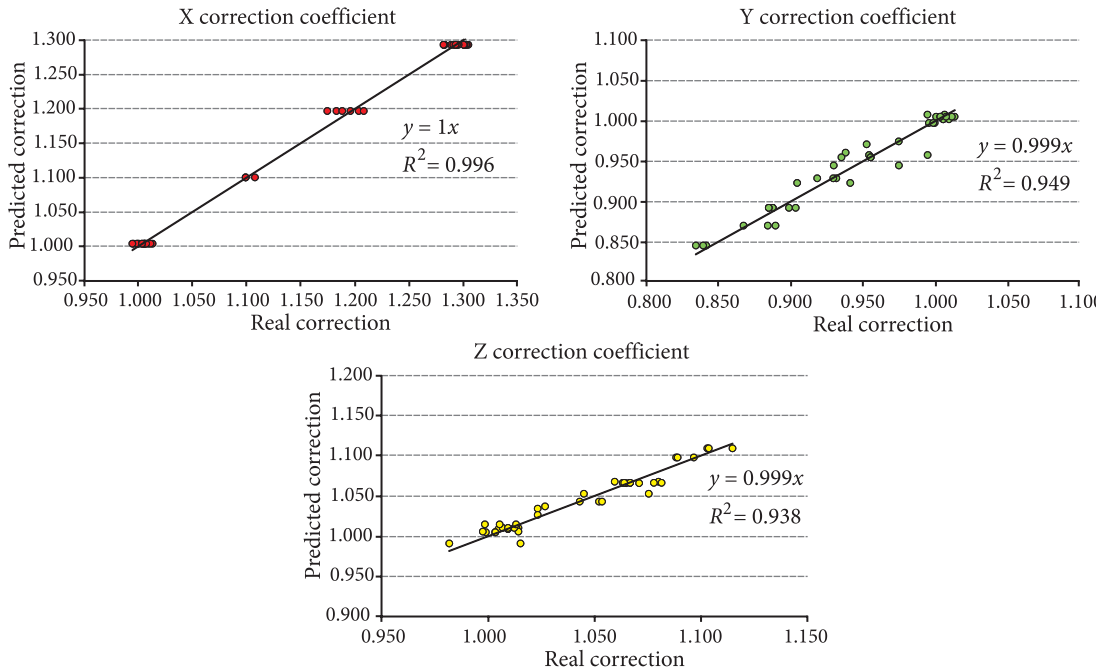

Fig. 2. Comparison between real and predicted correction coefficient of the footprint radius

Table 3. Load configurations for calculation of strains outside the footprint area

No.	Geometric conversion	Description
1.	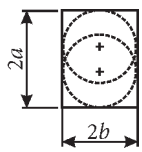	– 2 circles tangent to the edges of the rectangle; – same load P ($\frac{P}{2}$ for each circle).
2.	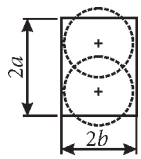	– 2 circles, barycentric in the semi-rectangles ; – same load P ($\frac{P}{2}$ for each circle); – same vertical stress, radius of the single circular footprint $r = \sqrt{\left(\frac{2ab}{\pi}\right)}$.
3.	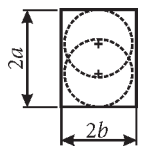	– 2 circles tangent to the short edges of the rectangle; – same load P ($\frac{P}{2}$ for each circle); – same vertical stress, radius of the single circular footprint $r = \sqrt{\left(\frac{2ab}{\pi}\right)}$.
4.	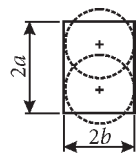	– 2 circles tangent to the long edges of the rectangle; – circles barycentric in the semi-rectangles ; – same load P ($\frac{P}{2}$ for each circle).
5.	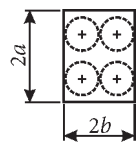	– 4 circles tangent two by two and to the long edges of the rectangle; – circles barycentric in the quarter rectangles ; – same load P ($\frac{P}{4}$ for each circle).
6.	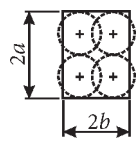	– 4 circles barycentric in the quarter rectangles; – same load P ($\frac{P}{4}$ for each circle); – same vertical stress, radius of the single circular footprint $r = \sqrt{\left(\frac{2ab}{\pi}\right)}$.

$$r_x = \sqrt{\frac{4ab}{\pi}}\left(0.714 + 0.290\frac{a}{b}\right), \quad (2)$$

$$r_y = \sqrt{\frac{4ab}{\pi}}\left(1.180 - \frac{a}{b}\left(0.462z^2 + 0.196\right) + \left(\frac{a}{b}\right)^2 0.208z\right), \quad (3)$$

$$r_z = \sqrt{\frac{4ab}{\pi}}\left(0.908 - \frac{a}{b}\left(0.889z^2 - 0.145\right) + \left(\frac{a}{b}\right)^2 \left(0.271z - 0.0639\right)\right). \quad (4)$$

The above formulas are valid for $a \geq b$. In the case $a < b$, the same formulas are used by changing r_x with r_y, a with b and viceversa.

Fig. 2 shows a comparison between correction coefficients λ_x, λ_y, λ_z, calculated by using formula (1) and those predicted by formulas (2), (3) and (4). As Fig. 2 shows, the proposed model provides an optimal approximation of the correction coefficient λ. The standard error of the estimate *Se* and the coefficient of determination R^2 are listed in Table 2. It was found that R^2 is very close to the unity and *Se* is very low.

3.2. Strains outside of the footprint area

The criterion of the equivalent single circular footprint cannot be extended to evaluate strains outside the footprint area. The results of simulations carried out by considering the equivalent single circular footprint for 15 combinations of the rectangular footprint size, depth z and mechanical properties of the elastic multilayer system, showed that a different approach has to be adopted for two reasons:

a) the correction coefficient λ to be applied to the circular footprint radius changes significantly as variable changes;

b) all other conditions being equal, the plot of strains versus y showed discontinuities and variations in convexity.

A different approach was thus adopted, based on the superposition of the effects produced by a series of circular footprints suitably distributed within the rectangular footprint. In this approach, the problem consists of defining the number of circular footprints, their radius, their position and the load to be assigned to each circular footprint in such a way as to obtain, for $y \neq 0$, the same strains as those produced by the rectangular footprint. Table 3 shows the feasible load configurations considered where P is the rectangular footprint load, kN, a and b are the lengths of the principal axles, m.

The results of simulations are reported in Fig. 3. It shows that the configuration No. 4 provides a good fit of ε_x plots versus the axis y; in addition, it points out that the configurations No. 5 and No. 6 well fit the plots of ε_y and ε_z values, respectively.

The load configurations allow to obtain a good fit of the strain plots outside the footprint area, whilst strains beneath the footprint are quite different. As expected, all the geometric configurations provide a good fit of strains far away from the footprint (for $y > 0.3$ m) demonstrating the load geometry has a negligible effect with increasing distance. For vertical strains, the fit is good even closer to the footprint (about 15 cm).

Fig. 4 shows some examples of a comparison between strain values calculated by using the rectangular footprint and values calculated by the circular footprint superposition at different distances y from the footprint centre.

The configurations obtained are valid for $a \geq b$. The conversions valid for $a < b$ are obtained by considering a 90° rotation of the footprint.

4. Conclusions

1. Although circular-shaped footprint is widely used in classical pavement design methods, it brings to considerable errors in both the stress-strain computation and the evaluation of rutting or cracking. The use of rectangular shaped footprints is certainly closer to the real geometry of the tire footprint but, despite this, it is not applicable to usual models of computation.

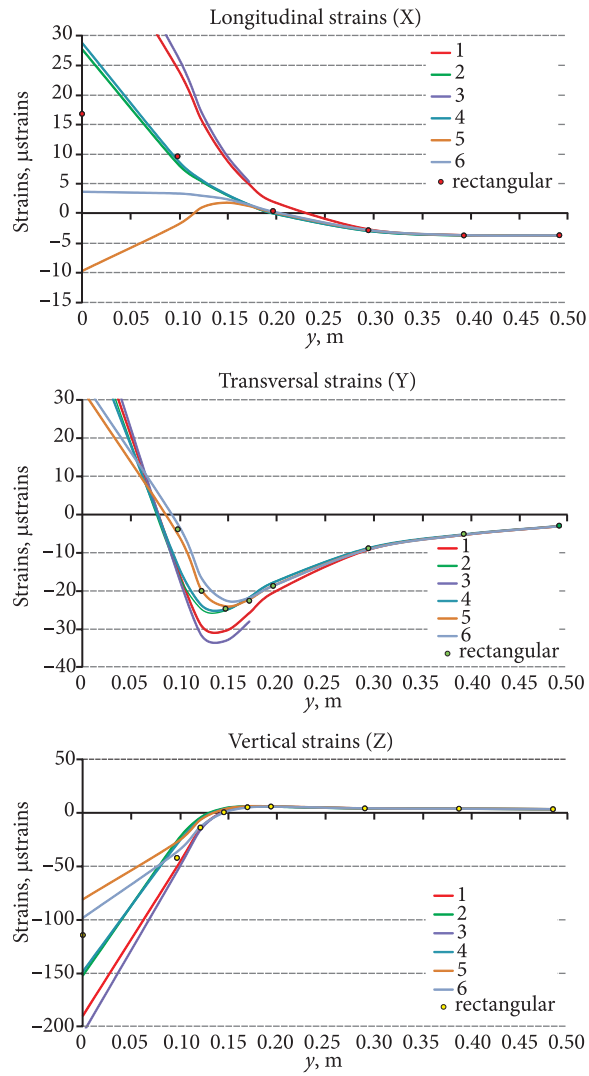

Fig. 3. Plots of strains versus y for different circular footprint super-positions and for a rectangular footprint

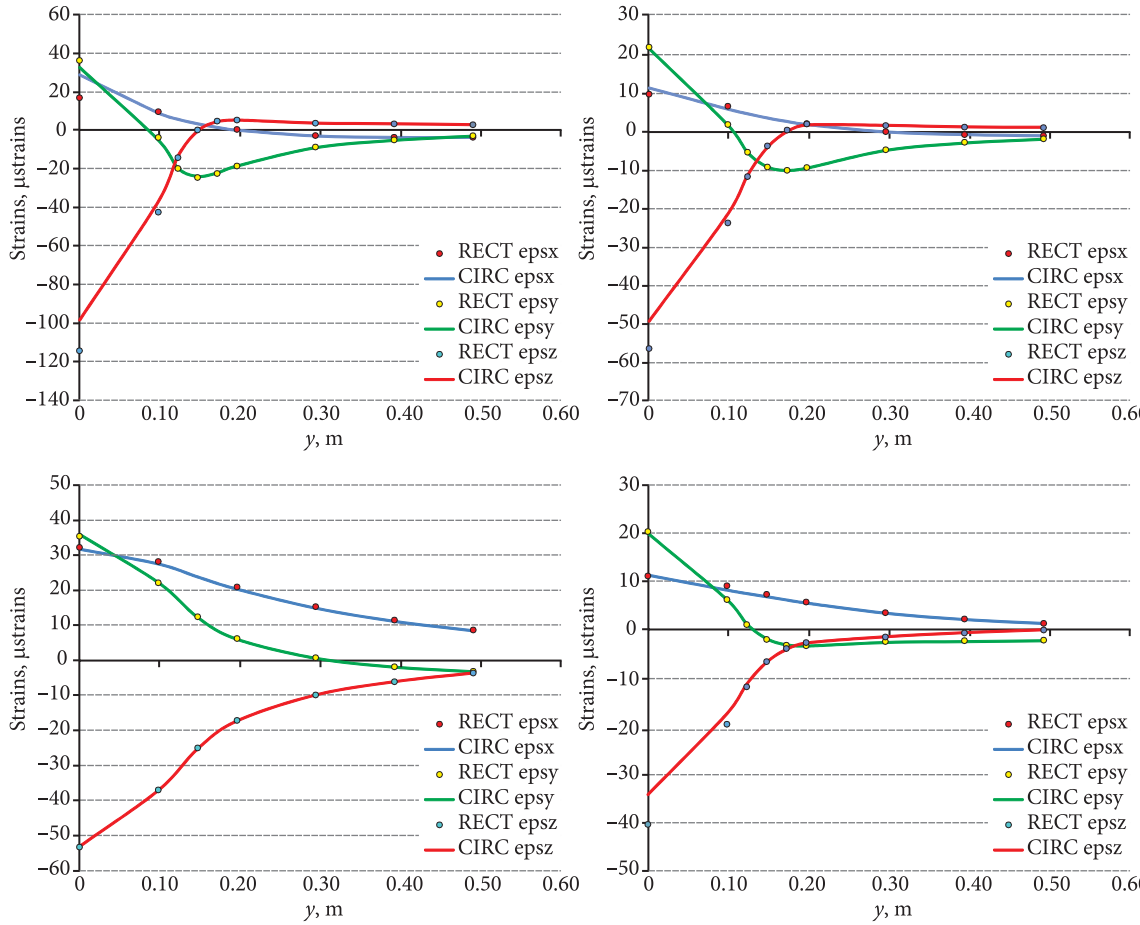

Fig. 4. Examples of the comparison between strains obtained with the circular footprint configurations chosen and strains calculated with the rectangular footprint

2. In order to estimate the difference in strains evaluated by using these two different geometric configurations, some simulations were carried out by an axial-symmetric linear elastic model and a 3*D* linear elastic model that allows taking into account rectangular footprints.

3. Subsequently, in order to convert a generic rectangular footprint into an equivalent single circular footprint or into a superposition of circular footprints, some equivalence relationships were determined. These two equivalent load configurations (single circular and superposition of circular footprints) produce the same strains in pavements both beneath the centre and outside of the loaded area.

4. The proposed relationships represent a useful tool that allows to consider the rectangular-shaped footprint which is closer to reality if compared to the circular one in evaluating the pavement response; at the same time, these relationships allow to benefit of the simplicity of the axial-symmetric linear elastic methods.

References

Alkasawneh, W.; Pan, E.; Green, R. 2008. The Effect of Loading Configuration and Footprint Geometry on Flexible Pavement Response Based on Linear Elastic Theory, *Road Materials and Pavement Design* 9(2): 159–179.

Blab, R. 1999. Introducing Improved Loading Assumptions into Analytical Pavement Models Based on Measured Contact Stresses of Tires, in *The International Conference on Accelerated Pavement Testing*, Reno, NV, 1999.

Chabot, A.; Chupin, O.; Deloffre, L.; Duhamel, D. 2010. A Tool for the Simulation of Moving Load Effects on Asphalt Pavement, *RMPD Special Issue on Recent Advances in Numerical Simulation of Pavements* 11(2): 227–250. http://dx.doi.org/10.3166/rmpd.11.227-250

De Beer, M.; Fisher, C. 1997. *Contact Stresses of Pneumatic Tires Measured with the Vehicle-Road Surface Pressure Transducer Array (VRSPTA) System for the University of California at Berkeley (UCB) and the Nevada Automotive Test Center (NATC).* CSIR Report CR-97/053. Council for Scientific and Industrial Research, Pretoria, South Africa.

Duhamel, D.; Chabot, A.; Tamagny, P.; Harfouche, L. 2005. Viscoroute: Visco-Elastic Modeling for Asphalt Pavements, *Bulletin des Laboratoires des Ponts et chaussées* 258–259: 89–103. Available from Internet: http://www.lcpc.fr/en/sources/blpc/index.php

Hajj, E.; Thushanthan, P.; Sebaaly, P. E.; Siddharthan, R. V. 2012. Influence of Tire-Pavement Stress Distribution, Shape, and Braking on Asphalt Pavement Performance Predictions, *Transportation Research Record* 2306: 73–85. http://dx.doi.org/10.3141/2306-09

Losa, M.; Di Natale, A. 2014. Accuracy in Predicting Visco-Elastic Response of Instrumented Asphalt Pavements, in *Proc. of the 3rd International Conference on Transportation Infrastructure (ICTI 2014). Sustainability, Eco-efficiency and Conservation in Transportation Infrastructure Asset Management.* April 22–25, 2014, Pisa, Italy, Taylor & Francis Group. 339–346.

Losa, M.; Di Natale, A. 2012. Evaluation of the Representative Loading Frequency in Asphalt Pavements, *Transportation Research Record* 2305: 150–161. http://dx.doi.org/10.3141/2305-16

Losa, M.; Bacci, R.; Leandri, P. 2008. A Statistical Model for Prediction of Critical Strains in Pavements from Deflection Measurements, *Road Materials and Pavement Design* 9(Supplement 1): 373–396. http://dx.doi.org/10.1080/14680629.2008.9690175

Novak, M.; Brigission, B.; And Roque, R. 2003. Tire Contact Stresses and Their Effects on Instability Rutting of Asphalt Mixture Pavements, *Transportation Research Record* 1853: 150–156. http://dx.doi.org/10.3141/1853-17

Park, D. W.; Fernando, E.; Leidy, J. 2005a. Evaluation of Predicted Pavement Response with Measured Tire Contact Stresses, *Transportation Research Record* 1919: 160–170. http://dx.doi.org/10.3141/1919-17

Park, D. W.; Martin, A. E.; Masad, E. 2005b. Effects of Nonuniform Tire Contact Stresses on Pavement Response, *Journal of Transportation Engineering* 131(11): 873–879. http://dx.doi.org/10.1061/(ASCE)0733-947X(2005)131:11(873)

Wang, F.; Machemehl, R. B. 2006. Mechanistic-Empirical Study of Effects of Truck Tire Pressure on Pavement: Measured Tire-Pavement Contact Stress Data, *Transportation Research Record* 1947: 136–145. http://dx.doi.org/10.3141/1947-13

Weissman, S. L. 1999. Influence of Tire-Pavement Contact Stress Distribution on Development of Distress Mechanism in Pavements, *Transportation Research Record* 1655: 161–167. http://dx.doi.org/10.3141/1655-21

Yue, Z. Q.; Svec, O. J. 1995. Effects of Tire-Pavement Pressure Distribution on the Response of Asphalt Concrete Pavements, *Canadian Journal of Civil Engineering* 22(5): 849–860. http://dx.doi.org/10.1139/l95-103

Received 20 December 2011; accepted 2 April 2012